

OMEGA EP

System Operations Manual

Volume VII–System Description

Chapter 2: Laser Sources

2.1	INTRODUCTION	1
2.2	REQUIREMENTS	4
2.3	SHORT-PULSE FRONT END.....	7
2.3.1	Short-Pulse Oscillator	7
2.3.2	Grating Pulse Stretcher	8
2.3.3	Optical Parametric Chirped-Pulse Amplification.....	9
2.3.4	OPCPA Pump Laser	13
2.4	LONG-PULSE FRONT END	14
2.4.1	Integrated Front-End Source	15
2.4.2	Temporal Pulse Shaping	15
2.4.3	Regenerative Amplifier	16
2.4.4	Stimulated Brillouin Scattering.....	17
2.5	COMMON FRONT-END STAGING.....	17
2.5.1	Spatial Beam Shaping	17
2.5.2	Glass Amplification.....	17
2.6	DIAGNOSTICS	17
2.6.1	Short-Pulse Oscillator	18
2.6.2	Optical Parametric Chirped-Pulse Amplification.....	18
2.6.3	Monomode Oscillator	18
2.6.4	Input Sensor Package	19
2.6.4.1	Temporal Pulse Shape	19
2.6.4.2	Spatial Beam Shape	19
2.6.4.3	Alignment Sensor Package.....	19

2.7	TIMING SYSTEMS AND FIDUCIAL LASER.....	20
2.7.1	Timing and Long-Pulse Fiducial.....	20
2.7.2	Precision Optical Timing Trigger System (POTTS).....	20
2.8	REFERENCES.....	22

APPENDIX A: GLOSSARY OF ACRONYMS

Chapter 2 Laser Sources

2.1 INTRODUCTION

The laser sources subsystem generates the shaped input pulses for the four beamlines. The first floor of the OMEGA EP Facility has an ~4500 ft², Class 1000 clean room located directly below the Laser Bay dedicated to the laser sources. Figure 2.1 provides an illustration of this arrangement. An injection periscope conveys the laser sources output pulse to the infrared alignment table (IRAT), located in the Laser Bay, where it is coaligned with the alignment laser. From the IRAT, the main pulse is transported to the injection table and injected into the beamline spatial filters and proceeds on to the amplifiers. The Laser Sources Bay contains all the equipment needed to create the laser beam that travels through the beamline amplifiers and to the target. Many of the critical beam characteristics are determined by the laser sources subsystems, including temporal, spatial, and spectral pulse shaping and energy. The pulse also meets the system wavefront, centering, and pointing budgets.

There are independent laser sources for each of the four beamlines (Fig. 2.2). Sources for Beamlines 1 and 2 produce both short (1- to 1000-ps) and long (1- to 10-ns) pulses (shown schematically in Fig. 2.3). Sources for Beamlines 3 and 4 provide only long-pulse beams and have similar but more-simple configurations (shown in Fig. 2.4). Short-pulse operations originate in a mode-locked oscillator that produces 200-fs pulses with a large spectral bandwidth. These pulses are stretched in time (chirped) and amplified using optical parametric chirped-pulse amplification (OPCPA).^{1,2} Long pulses from all laser sources beams originate in a single-frequency fiber laser and are amplified in a regenerative amplifier

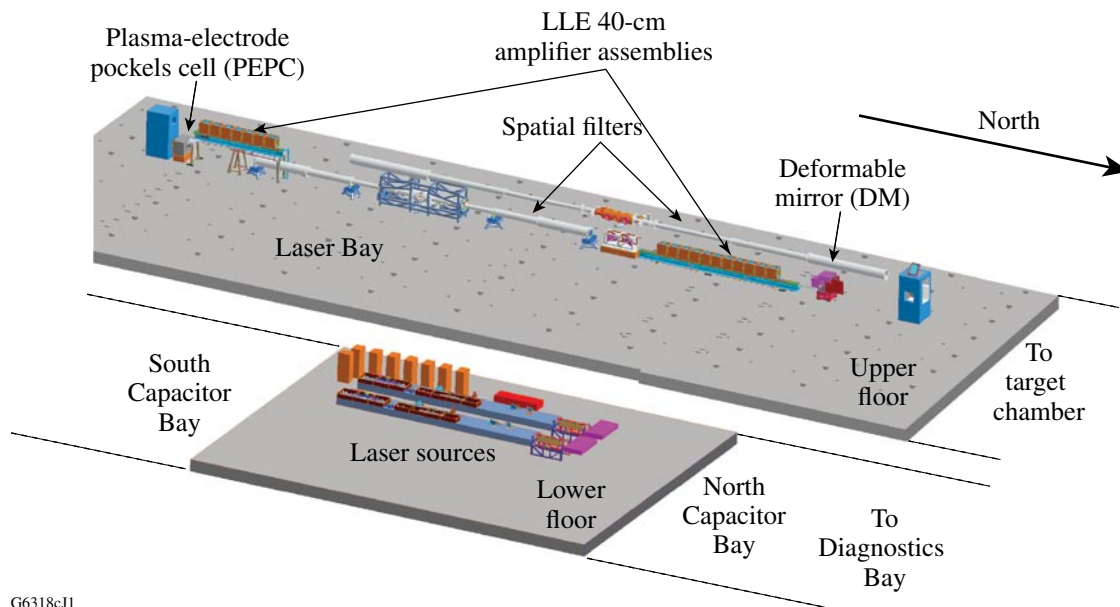


Figure 2.1

Laser sources are located in a clean room directly below the Laser Bay between the South and North Capacitor Bays. Only one Laser Bay beamline and two laser sources are shown for clarity.

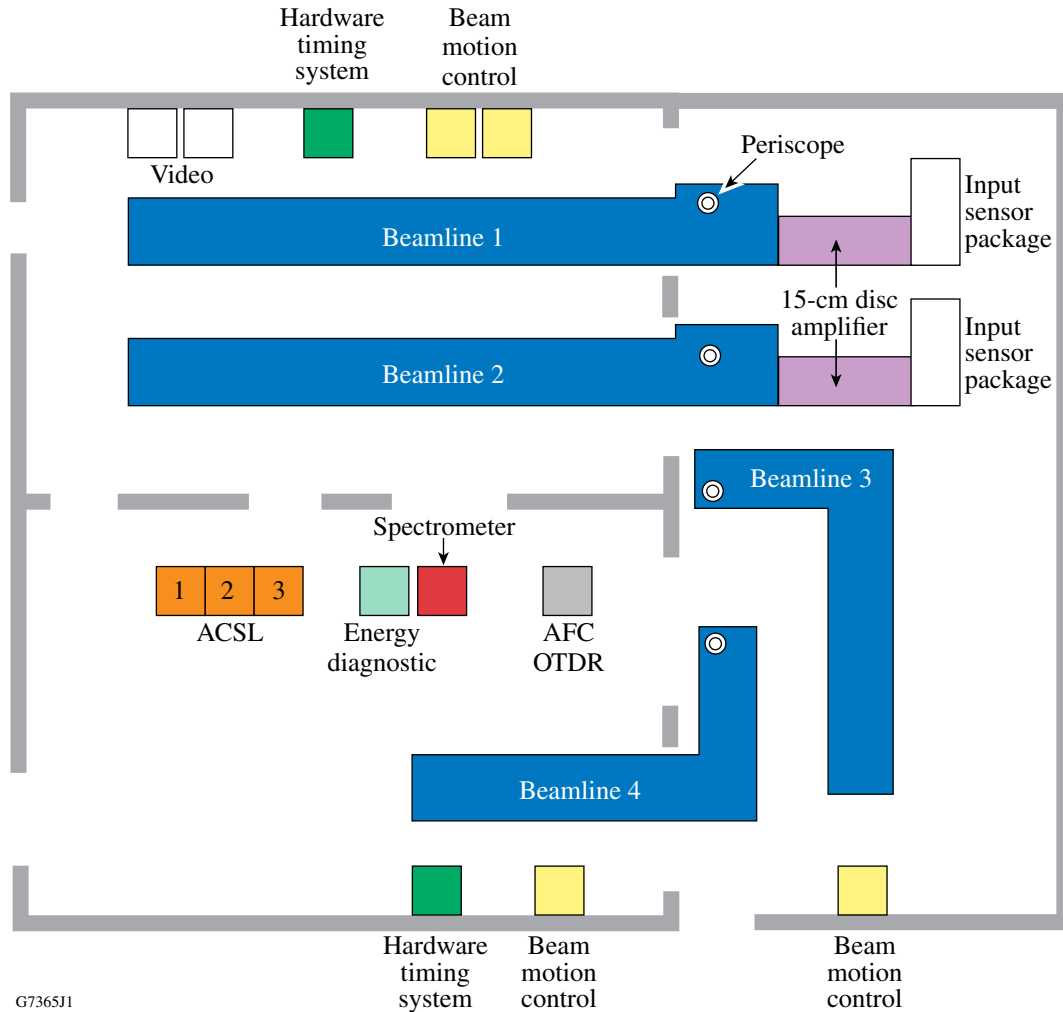


Figure 2.2

Simplified Laser Sources floor plan. Each of the four beamlines is supported by an independent source (blue). The 15-cm disc amplifiers and input sensor package positions are shown for Beamlines 1 and 2. The locations of other supporting diagnostic and control equipment are also shown.

(regen) after temporal shaping. The long-pulse regen pulse “on beams 1 or 2” requires an additional double-pass preamplifier stage to raise the energy to the levels required for sharing the remaining path of the laser sources chain with the short OPCPA pulses. Either pulse is then passed through a glass amplifier (Fig. 2.4) that boosts the energy to the required levels for the beamline amplification stages. Each type of pulse must satisfy different sets of design requirements for its spatial intensity distribution, temporal pulse shape, and spectral composition.

The top-level source requirements are presented in Sec. 2.2, followed by a more detailed discussion of the short-pulse and long-pulse front ends (Secs. 2.3 and 2.4, respectively) and subsystems common to both front-end configurations (Sec. 2.5). Many of the subsystem components are based on technologies currently in use on the OMEGA system. Examples include single-frequency fiber lasers, aperture-coupled strip line (ACSL) pulse-shaping systems,³ diode-pumped regenerative amplifiers,⁴ and bulk electro-optic phase modulators⁵ that apply a frequency-modulated (FM) bandwidth to the laser pulses. Finally, Sec. 2.6 provides an overview of the diagnostics required to monitor the performance of the laser sources.

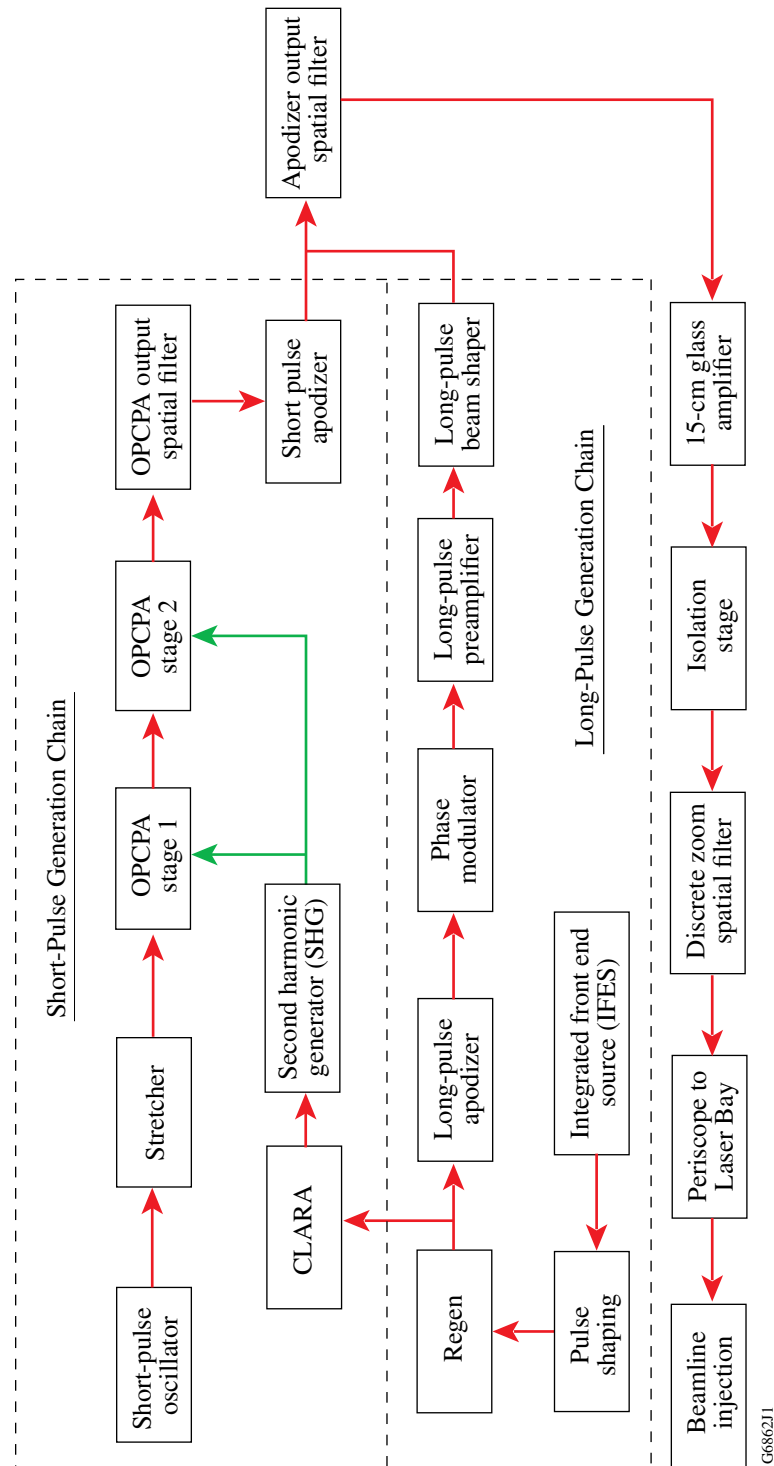


Figure 2.3

Schematic diagram of the Laser Sources subsystem design for Sources 1 and 2. These sources support both short-pulse (1 to 100 ps) and long-pulse (1 to 10 ns) operation. The “green” coloration from the CLARA SHG indicates 2ω . Beamlines 3 and 4 do not have short-pulse capability and therefore have a different configuration.

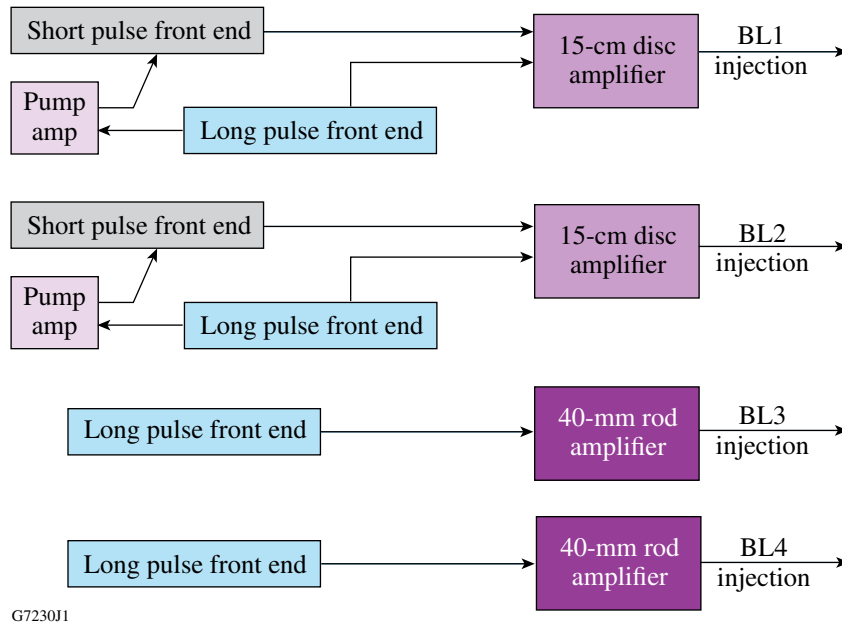


Figure 2.4

Simplified schematic of laser sources' top-level design configurations. The laser sources' configuration of Beamlines 1 and 2, which can support a short or long pulse, is slightly more complex than that of Beamlines 3 and 4, which provide pulses only for long pulse.

2.2 REQUIREMENTS

OMEGA EP's laser sources subsystem contains six separate laser systems for injecting pulses into the main beamlines, four for long-pulse operation and two for short-pulse operation. The laser sources final component in each beamline is the periscope leading from the Laser Sources Bay to the beamline's IRAT. These optical periscopes transport the pulses to the injection system near the focal plane of the transport spatial filter (TSF) located in the Laser Bay. The requirements for the short-pulse front-end laser sources are listed in Table 2.1.

Referring to Fig. 2.3, a 76-MHz, 200-fs, mode-locked seed oscillator, synchronized to a hardware timing system (HTS), 76-MHz electrical signal, supplies pulses to an all-reflective grating pulse stretcher (one pulse every 13 ns). The stretcher output is spatially shaped and amplified at a modest repetition rate (5 Hz) to 250 mJ in a broadband amplifier employing OPCPA. Subsequent pulse amplification occurs in a four-pass, Nd-doped, phosphate glass amplifier. Gain narrowing in the glass amplifier reduces the chirped-pulse bandwidth from ~8 nm to ~6 to 7 nm full-width at half-maximum (FWHM). This amplifier is common to both the long-pulse and short-pulse front ends. The long-pulse front-end system is based on technology in use at both Lawrence Livermore National Laboratory (LLNL)⁶ and LLE⁷ and provides up to four independent sources of independently timed, temporally shaped FM pulses for injection into the main beamlines. The system requirements for the long-pulse front end are shown in Table 2.2. The front-end output energy is pulse-shape dependent within the pulse-width range of 1 to 10 ns. FM bandwidth is applied to suppress stimulated Brillouin scattering (SBS) in the large-aperture final optics.⁸

Table 2.1: Short-pulse injection requirements.

Number of sources	2
Pulse energy	0.07 → 3.9 J (nonapodized)
Spatial pulse shape	Appropriate to compensate the nonuniform gain in the main amplifiers with less than 20% P-M spatial modulation with respect to Fig. 2.5.
Beam size	$58.6 \times 58.6 \text{ mm}^2$; FW 1%
Relative timing to other OMEGA and OMEGA EP pulses	Independently timed jitter ≤ 10 -ps rms
Stretch ratio	300 ps/nm
Stretch-ratio range	$-40 \text{ ps/nm} \rightarrow +20 \text{ ps/nm}$
Spectral bandwidth	$>6 \text{ nm}$ (FWHM)
Central wavelength	1053 nm
Tolerance	$\pm 0.5 \text{ nm}$
<i>B</i> -integral	$<0.20 \text{ rad}$
Wavefront divergence	$<3.5 \mu\text{rad}$ ($22.05 \mu\text{rad}$ @ full beam size)
Pointing stability (p-v)	$<5 \mu\text{rad/h}$
Centering specification	$\pm 0.17\%$
Output isolation	$>25 \text{ dB}$

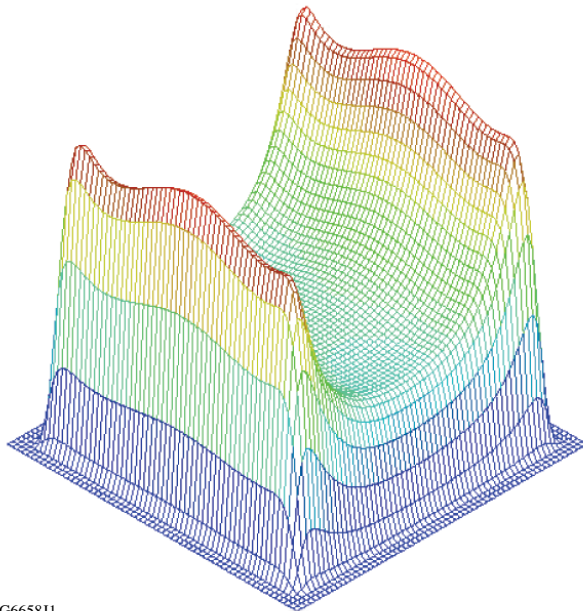


Figure 2.5

The spatial profile of the beam must precompensate the spatial gain nonuniformities in the main amplifiers such that a flattop beam shape is produced at the input of the pulse compressor.

Table 2.2: Long-pulse front-end laser-source requirements.

Number of sources	4
Pulse energy	>0.575 J @ 2 ns (without beam shaping) >3.5 J @ 10 ns (without beam shaping)
Temporal pulse width	1 to 10 ns FW 1%
Pulse-shaping intensity contrast	50:1 (see Fig. 2.6)
Relative timing to other OMEGA and OMEGA EP pulses	Independently timed, jitter 10-ps rms
Wavelength Tolerance	1053.04 nm ± 0.03 nm
Spatial pulse profile	Appropriate for compensation of nonuniform gain in the main amplifiers
Beam size	58.6×58.6 mm ² ; FW 1%
Wavefront divergence	< 3.5 μ rad
Pointing stability (p-v) Centering specification	< 5 μ rad/h $\pm 0.17\%$
Phase modulation – spectrum – bandwidth	FM modulated (>10 sidebands) $\Delta\lambda = 1$ Å

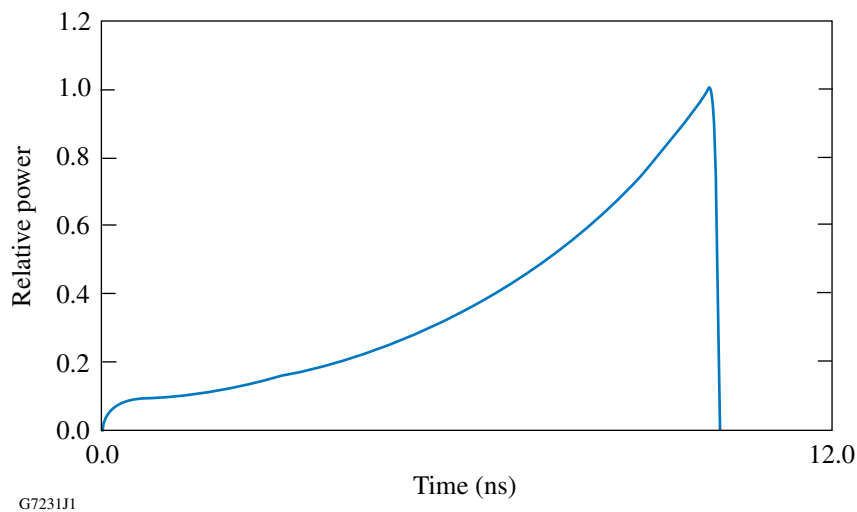


Figure 2.6

Example of a normalized temporal pulse shaper required at the injection plane for a 10-ns pulse. The lower foot of the pulse precompensates the gain effects of the glass amplifiers.

2.3 SHORT-PULSE FRONT END

This section describes the subsystems that are utilized when a short pulse is propagated through the main amplifiers. These include the mode-locked oscillator and switch-out Pockels cell, grating pulse stretcher, and OPCPA system, including the OPCPA pump laser.

2.3.1 Short-Pulse Oscillator

A continuous train of ~ 220 -fs laser pulses is generated by a commercial, mode-locked, Nd-doped glass laser. Hybrid mode-locking produces an approximately transform-limited laser pulse that is synchronized to the OMEGA HTS with a low jitter (< 10 ps). A schematic diagram of this oscillator is shown in Fig. 2.7, and the performance requirements are listed in Table 2.3.

A semiconductor-saturable absorbing mirror (SESAM) used as the cavity end mirror provides the passive mode-locking mechanism that produces the ultrashort pulses.⁹ The active mode-locking mechanism, which synchronizes the pulse timing to OMEGA, is accomplished with the SESAM coupled to a motorized precision translation stage with a piezoelectric transducer (PZT). A 76-MHz reference signal drives the PZT mirror mount with a sinusoidal signal, which FM mode-locks the laser cavity and synchronizes the laser pulses to the reference signal. Stable mode-locking requires the cavity round trip time to match the period of the mirror oscillations (~ 13 ns). The output of a leaky mirror provides feedback to a timing stabilizer system that compares the relative phase of the clock signal to the feedback signal and matches the laser cavity length to the period of the 76-MHz reference signal. Small adjustments are accomplished with the PZT, while larger adjustments require translating the PZT-mounted SESAM

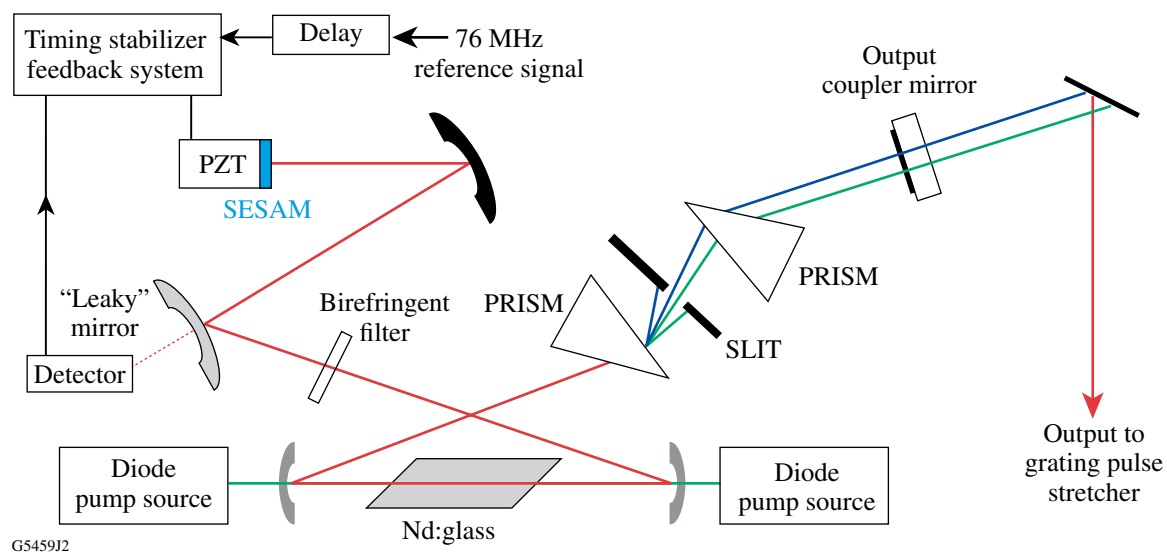


Figure 2.7

Block diagram of the short-pulse oscillator. The active medium is diode-pumped Nd:glass. Synchronization is provided through the SESAM. Spectral tuning is obtained using a prism pair and an adjustable slit that determines which wavelengths experience low loss.

Table 2.3: Performance requirements of principal oscillators.

	IFES laser	Short-pulse oscillator	OPCPA pump laser
Number of lasers	4	2	2
Oscillator type	Monomode	Mode-locked	Monomode
Active medium	Nd:YLF	Nd:glass	Nd:YLF with SHG
Central wavelength	1053 nm	1053 nm	526.5 nm
Output energy	~150 nJ	>1 nJ	>2 J
Amplitude stability (rms)	1%	1%	1%
Wavelength stability (p-v)	0.03 nm/24 h	0.5 nm/h	N/A
Pulse duration (FWHM)	20 ns	220 fs	2 to 3 ns
Spectral width	SLM ^(a)	>8 nm	SLM ^(a)
Temporal jitter	20 ps	≤1-ps rms	<300 ps
Repetition rate	300 Hz	76 Mhz	5 Hz
^(a) The requirement is single longitudinal mode (SLM).			

assembly. The Nd:glass amplifier provides gain at the desired 1053-nm center wavelength with a large gain bandwidth for mode-locking. An intracavity prism pair provides dispersion compensation and, in conjunction with a birefringent filter, controls the operating wavelength and bandwidth of the laser output. A Pockels cell is used after the oscillator to switch out a single pulse at a 5-Hz repetition rate, to provide isolation that keeps prepulse noise on target minimized, and protects against light leaking back from the grating pulse stretcher.

2.3.2 Grating Pulse Stretcher

A frequency-chirped laser refers to a spectral spreading out of a broad-bandwidth short pulse through an arrangement of beam expanders and gratings. These optics are designed to spread the spectrum in time, resulting in a pulse of light where the color changes from the beginning of the pulse to the end. The output of the seed oscillator is temporally stretched in a conventional double-pass, single-grating, all-reflective Offner triplet stretcher.^{10,11} The Offner triplet design is free from third-order aberrations, asymmetric Seidel aberrations, and chromatic aberrations. This scheme provides an adjustable chirp of 280 to 320 ps/nm, which yields an ~2.4-ns (FWHM) stretched pulse corresponding to the 8-nm input bandwidth. The net transmission of this stretcher is ~25%. To support the experimental program, the on-target pulse width of the short-pulse beams must be adjustable between 1 and 100 ps. The Offner triplet stretcher design provides a convenient approach to providing this system flexibility. Adjustment of the stretch ratio is realized by changing the separation between the grating and the optical system comprising the primary and secondary mirrors. Adjustment over an ~15-cm range provides the required range of pulse-width adjustment without requiring any changes to the gratings in the grating compressor chamber.

2.3.3 Optical Parametric Chirped-Pulse Amplification

OPCPA^{1,2} offers many advantages for front-end amplification in high-peak-power lasers, including large gain bandwidth, very high gain in a single pass with the associated advantage of a low B -integral, and improved prepulse contrast. The large gain bandwidth available with type-I optical parametric amplifiers makes it possible to maintain the bandwidth of the input pulse, thus allowing short pulses and high peak powers to be obtained upon pulse compression. The single-pass architecture afforded by OPCPA eliminates the leakage prepulses frequently associated with a multipass regenerative amplifier. Additionally, lower prepulse intensity levels after compression are possible with OPCPA because the parametric fluorescence (the amplification of noise in the OPCPA crystals) is lower than the corresponding amplified spontaneous emission produced by conventional laser amplification schemes that provide comparable gain. The parametric fluorescence is also confined to the temporal window of the pump laser.¹

The OPCPA system for OMEGA EP uses three type-I nonlinear optical crystals in the preamplifier and power amplifier stages, as shown schematically in Fig. 2.8. Lithium triborate (LBO) is used because of its high nonlinear coefficient, large angular acceptance, and small pump-beam walk-off angle. The pump laser produces temporally and spatially flattop pulses that are image relayed to the preamplifier and power-amplifier stages, as described in Sec. 2.3.4. A slight noncollinearity between the pump and the input signal beam permits separation of the OPCPA output signal and idler beams with apertures. The pump intensity at each crystal is limited to approximately 1 GW/cm^2 to avoid laser-induced damage of the crystals or their antireflective coatings. Computer simulations performed using a three-dimensional numerical model for this design predict a signal output energy of 558 mJ with 40% overall conversion efficiency relative to the pump laser, not including passive losses from optical components in the propagation path (Fig. 2.9). Input and output parameters for this design are given in Tables 2.4 and 2.5, respectively.

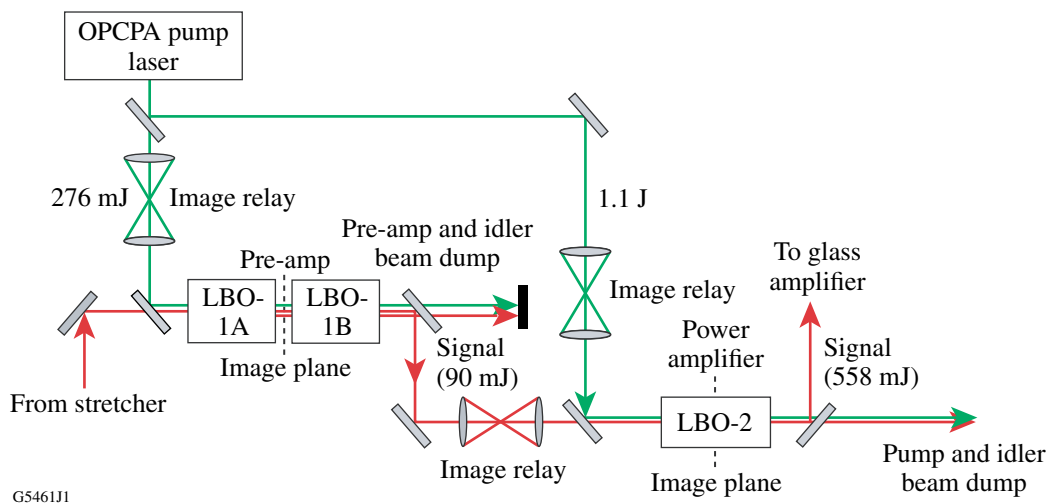


Figure 2.8

Two-stage, three-crystal LBO configuration of the OMEGA EP OPCPA front end. This design provides 558 mJ of signal energy at 1053 nm with an overall pump-to-signal conversion efficiency of 40% for injection into the front-end Nd:glass amplifier. Note: green lines are 551 nm and red lines are 1053 nm.

The first two crystals of the OPCPA system comprise a preamplifier stage that is designed for both high-efficiency and high-output energy stability, as indicated in Table 2.5. Extremely high gain is produced in the first preamplifier crystal with little pump depletion, while additional gain and significant conversion efficiency are realized in the second crystal. The pump and signal energies are plotted in Fig. 2.9 versus the propagation distance in the second LBO preamplifier crystal (LBO-1B). Enhanced signal output energy stability is obtained when the crystal lengths are chosen such that the OPCPA system is operated just past the peak of its gain curve.¹² As seen in Fig. 2.10, this regime of operation is achieved using 29.75-mm-long LBO crystals. Pump depletion and reconversion in the preamplifier OPCPA stage reduce the sensitivity of the signal-pulse output energy to pump energy fluctuations,¹² but they also distort the spatiotemporal shape of the signal pulse since different portions (spatial and temporal) experience varying degrees of gain and/or reconversion. Optimizing the preamplifier crystal lengths and the pump intensity balances these competing effects.

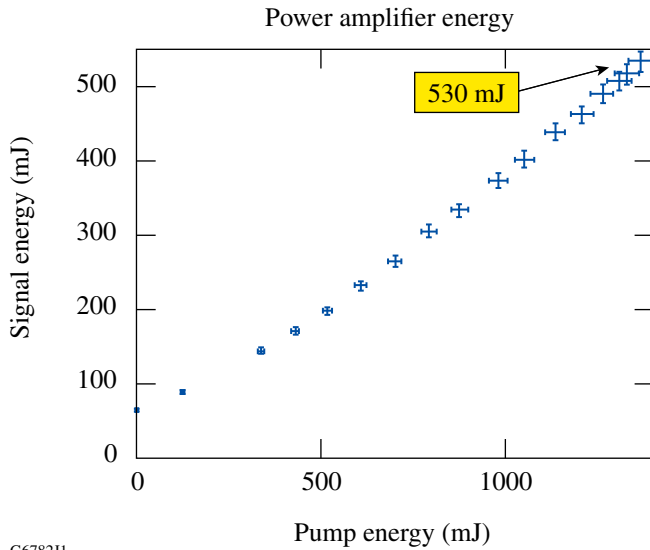


Figure 2.9
OPCPA output energy readily achieves the 250-mJ pulse energy and is controlled by the pump energy.

G6782J1

Table 2.4: Input parameters for the OMEGA EP OPCPA design. Spatial profiles of the form $\exp[(r/r_0)^n]$ are assumed, where n is the spatial order. The temporal order is similarly defined.

		Preamplifier		Power amplifier
Crystal		LBO-1A: 29.75 mm LBO-1B: 29.75 mm		LBO-2: 11.0 mm
		Seed	Pump	Pump
Energy		100 pJ	276 mJ	1.1 J
Beam width (FWHM)	X	3.2 mm	3.4 mm	6.8 mm
	Y (walk-off direction)	3.2 mm	3.4 mm	6.8 mm
Spatial order n		2	10	10
Temporal pulse width (FWHM)		2.4 ns (stretched)	2.4 ns	2.4 ns
Temporal order n		2	10	10

Table 2.5: Signal-beam output parameters for the OPCPA design given in Table 2.3.

	Preamplifier		Power amplifier
	LBO-1A	LBO-1B	LBO-2
Energy	2.9 μ J	90 mJ	558 mJ
Gain	2.90×10^4	3.10×10^4	6.2
Cumulative gain	2.90×10^4	9.0×10^8	5.58×10^9
Beam FWHM (X)	2.8 mm	3.1 mm	6.8 mm
Beam FWHM (Y)	2.8 mm	3.1 mm	6.8 mm
Temporal FWHM	1.8 ns	2.3 ns	2.3 ns
Bandwidth	6.3 nm	7.9 nm	7.9 nm
Spatially integrated temporal noise(a) (rms)	8.8%	2.8%	2.1%
Temporally integrated spatial noise(b) (rms)	18.7%	5.9%	3.2%
Conversion efficiency	0.001%	32.6%	42.6%
Pump depletion	0.12%	64.6%	85.4%
Overall signal output energy			558 mJ
Overall conversion efficiency			40.6%
Overall gain			5.6×10^9
(a)Input pump temporal noise is 3% rms.			
(b)Input pump spatial noise is 3.9 % rms.			

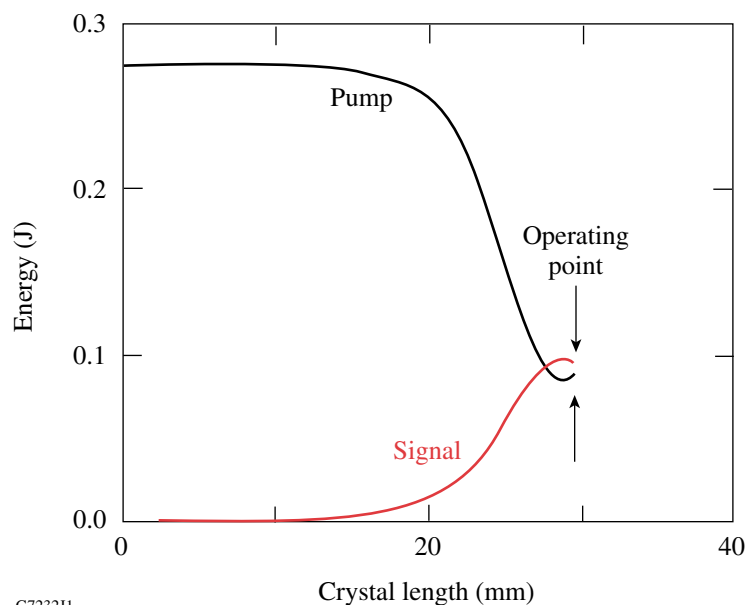


Figure 2.10

Pump and signal energy as a function of propagation distance in the second preamplifier crystal (LBO-1B). The crystal lengths are chosen such that the preamplifier operates just past the peak of its gain curve, thus providing enhanced energy stability.

A power-amplifier stage with a single LBO crystal provides the final amplification required to achieve 250-mJ signal-pulse energies. High conversion efficiencies are achieved by optimizing the pump intensity. The transfer of temporal and spatial intensity perturbations to the signal output beam is examined. Heavy pump depletion in the power-amplifier design reduces the influence of temporal and spatial fluctuations in the pump, as seen in Figs. 2.11 and 2.12. The resulting output signal pulse resembles a smoothed replica of the pump pulse shape. The LBO-based OPCPA baseline design illustrated in Fig. 2.8 and Tables 2.4 and 2.5 provides a robust approach to meeting the requirements shown in Table 2.1. The design also includes sufficient margin to accommodate real system performance limitations.

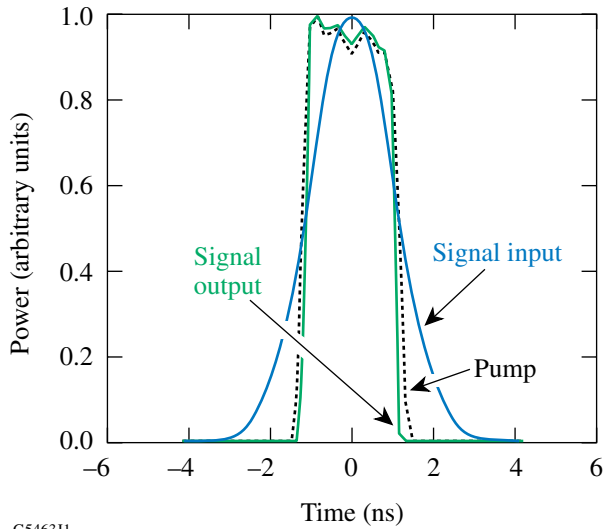
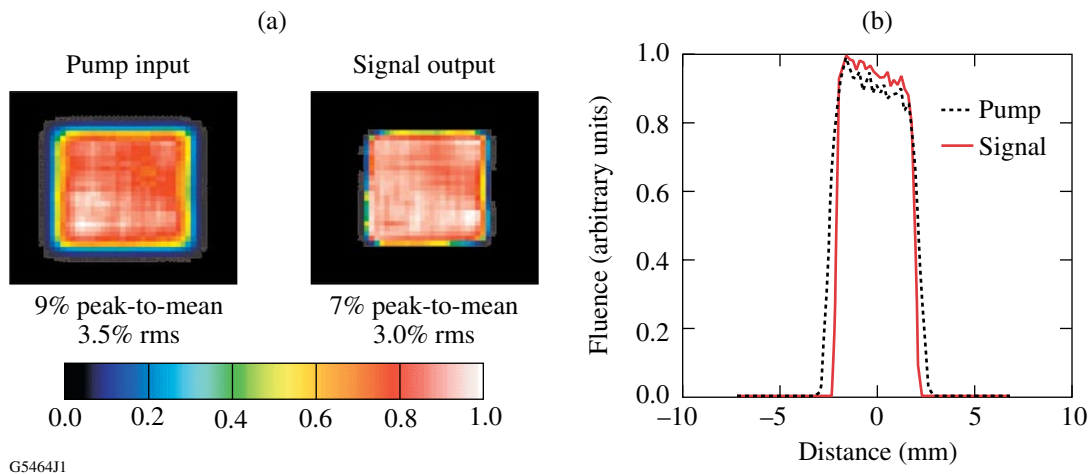


Figure 2.11
Normalized temporal profiles of the input pump and signal input/output pulses for the baseline design. The seed pulse entering the first crystal of the preamplifier is shown dotted, and the signal beam out of the power amplifier crystal is shown solid. The pump input temporal noise is 9% peak-to-valley (3% rms), whereas the amplified signal-output temporal noise is only 7% peak-to-valley (2% rms).

G5463J1



G5464J1

Figure 2.12
(a) Normalized beam cross sections for the temporally integrated pump input and the power amplifier signal output beams for the OMEGA EP OPCPA design. (b) Normalized horizontal lineouts through the center of each of the beams are shown in (a).

2.3.4 OPCPA Pump Laser

Successful operation of the OPCPA system described in Sec. 2.3.3 depends critically on the performance of the OPCPA pump laser. Many characteristics of the pump laser transfer to the amplified signal beam, including the spatial- and temporal-intensity profiles. The pump-beam energy, pointing, and wavelength stability are also significant factors in the OPCPA process, as are wavefront quality and timing jitter, since parametric processes are sensitive to pump fluctuations. The top-level pump-laser performance requirements necessary to achieve the OPCPA design are listed in Table 2.3.

The 2-J pump energy and 5-Hz repetition rate are primarily driven by the 250-mJ OPCPA output pulse energy required for aligning the final compressors. Efficiently amplifying chirped pulses with an 8-nm bandwidth requires a pump-laser pulse duration of 2.4 ns. Significant system simplification is realized by using most of the long-pulse front-end laser subsystems in the OPCPA pump laser, since the two modes of operation are not used simultaneously. As indicated in Fig. 2.3, the integrated front-end source (IFES) (Sec. 2.4.1), temporal pulse-shaping system (Sec. 2.4.2), and diode-pumped regenerative amplifier (Sec. 2.4.3) are used. This simplification requires the OPCPA pump-laser fundamental wavelength to be 1053 nm.

Two additional OPCPA pump-laser subsystems are required to meet the 5-Hz, high-pulse-energy requirement and provide frequency doubling. They are shown schematically in Fig. 2.3. The first subsystem is a Nd:YLF version of a large-aperture ring amplifier known as a crystal LARA (CLARA) and the other is a potassium dihydrogen phosphate (KDP) crystal used for second-harmonic generation.

The CLARA is used to amplify the laser pulse to a high energy (~2 J at 1053 nm) while minimizing temporal and spatial distortions. This multipass scheme also occupies a relatively small space and limits the amount of laser and power conditioning equipment required. The CLARA design is illustrated in Fig. 2.13. It uses two large-diameter (25-mm), flash-lamp-pumped, Nd:YLF crystals. The crystal axes of the two rods are oriented orthogonally to each other to prevent lasing on the 1064-nm YLF line. The CLARA output pulses are efficiently frequency doubled using a single crystal of KDP after setting the beam size for optimal conversion with a vacuum spatial filter. High-efficiency second-harmonic generation, approximately 66%, is achieved because of the flattop temporal and spatial profiles. High-contrast separation of the second harmonic from the residual fundamental light is required to avoid seeding the OPCPA stages. A large Pellin–Broca prism¹³ with a subsequent aperture provides the separation required. A half-wave plate and a polarizing beam splitter separate the pump pulse into two portions that are relay imaged to the two OPCPA amplifier stages with an appropriate energy for each stage. Relay imaging preserves the high-order super-Gaussian spatial profile required for maximum OPCPA conversion efficiency and minimizes intensity perturbations on the pump beam that could be transferred to the seed beam and exponentially amplified in the preamplifier.

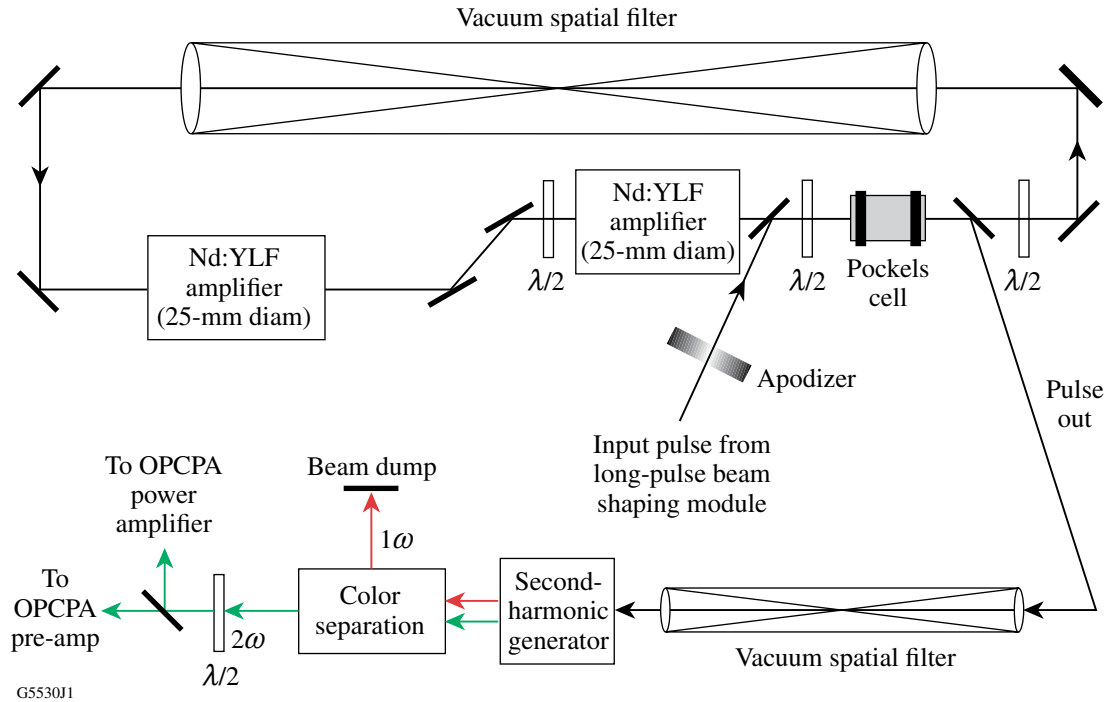


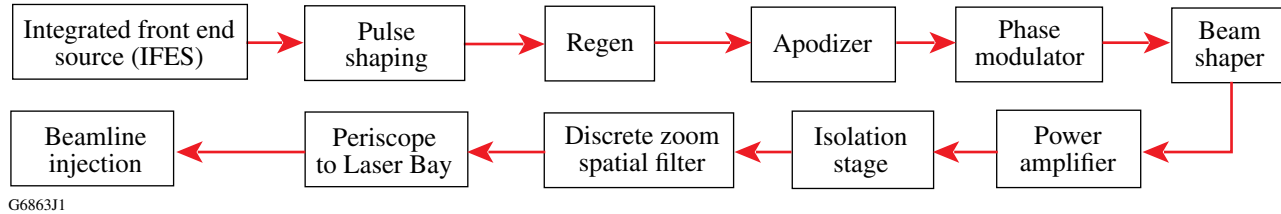
Figure 2.13
Schematic of a crystal large-aperture ring amplifier used as a power amplifier for the OPCPA pump laser. The CLARA design is very similar to the large-aperture ring amplifier design that is successfully utilized on OMEGA.

2.4 LONG-PULSE FRONT END

This section describes the subsystems that are utilized when a long pulse is propagated through the main amplifiers, including the integrated front-end source (IFES), the regenerative amplifier, and the phase modulator. With the exception of the phase modulator, these subsystems also serve as the front end of the OPCPA pump laser described in Sec. 2.3.4 above.

In long-pulse mode, the pulse lengths are adjustable between 1 and 10 ns. A schematic diagram of the system is shown in Fig. 2.14. The laser pulse originates from an IFES that contains a fiber laser. The fiber laser produces a continuous-wave output that is subsequently shaped so that the desired on-target temporal profile is generated. The pulse-shaping system uses arbitrary-waveform-generator (AWG) technology instead of the OMEGA-like aperture-coupled stripline (ACSL). The temporally shaped pulse is amplified in a regenerative amplifier that amplifies laser pulses at a 5-Hz rate. An apodizer shapes the spatial profile of the beam from round to square, creating an optimized, on-target, spatial profile. A small amount of frequency-modulation bandwidth is imposed to suppress stimulated Brillouin scattering⁸ that could otherwise threaten large optics such as the focus lenses. The bandwidth is applied at a modulation frequency using a bulk microwave lithium niobate (LiNbO_3) modulator. The pulse is further amplified in a glass amplifier* before injection into the beamlines' transport spatial filter. The optical-image plane of the long-pulse (LP) apodizer is relayed down the beamline.

*The 15-cm amplifiers are used in beamlines 1 and 2. The 40-mm rod amplifiers are used in beamlines 3 and 4 (Fig. 2.4)



G6863J1

Figure 2.14
Functional diagram of the long-pulse front end.

2.4.1 Integrated Front-End Source

The laser beam originates in a highly stable continuous-wave Bragg fiber laser. It is a commercial off-the-shelf laser that has a natural single-frequency operational mode. The fiber laser puts out 5 mW of 1054.04-nm laser light, which is fiber coupled to the pulse-shaping system. The laser conforms to the specifications listed in Table 2.6.

The output characteristics of this laser subsystem are summarized in Table 2.3.

Table 2.6: Bragg fiber laser specifications.

Wavelength (air)	1053.04 nm
Wavelength stability	<0.03 nm/24 h
Maximum power output	≥12 mW
Power stability	<1% rms over 2 h
Slow-axis polarization extinction ratio	≥100:1

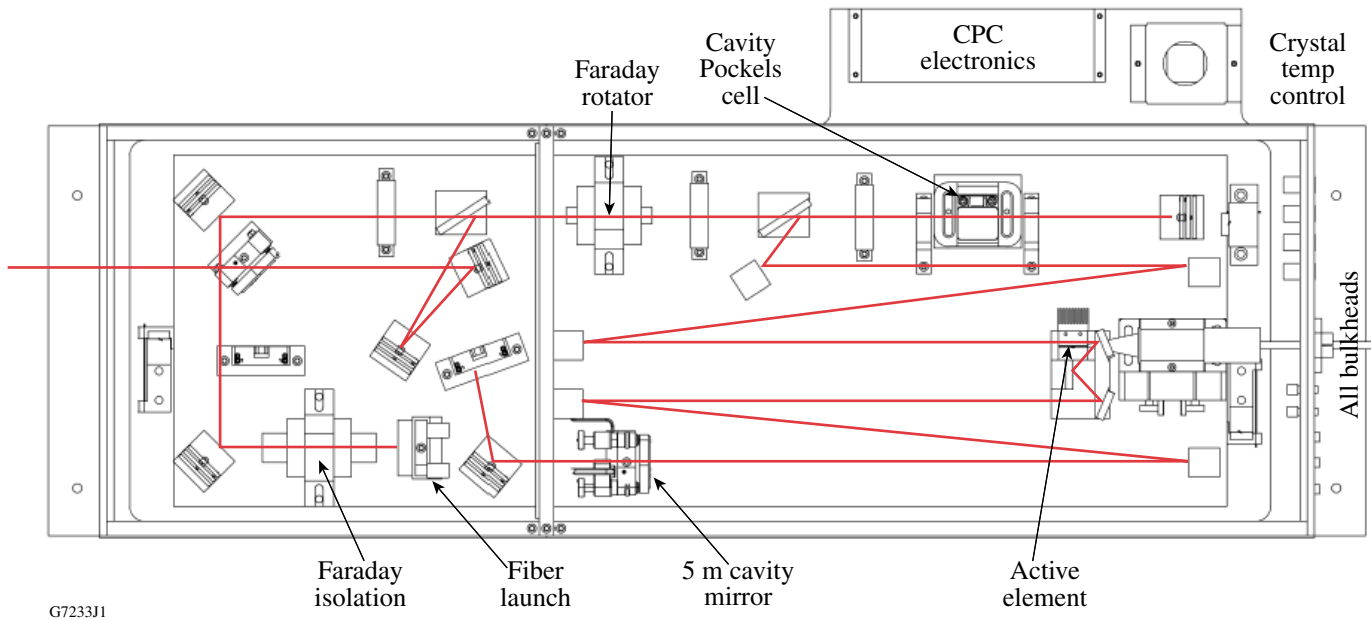
2.4.2 Temporal Pulse Shaping

The long-pulse system provides a wide range of temporal pulse shapes and lengths. Pulse shaping is applied before any amplification and compensates for pulse distortion caused by saturation in the amplifiers and nonlinear frequency-conversion effects. The pulse-shaping system combines elements of the ACSL system developed for OMEGA³ with a commercial AWG. Pulse shaping is accomplished using two amplitude modulators in series to provide optical gating and shaping functions. Each modulator is a LiNbO₃, integrated-optic, Mach-Zehnder interferometer in which the relative phase of the light between the legs can be controlled to produce the desired output amplitude after recombination. The optical path lengths are biased for minimum transmission such that an electrical pulse applied to the input increases transmission. The voltage pulse applied to the first modulator is a square pulse of a length that is determined by the desired total optical pulse duration. A shaped electrical pulse is applied to the second modulator to produce the desired optical pulse shape. The amplitude modulator chassis includes bias-pulse generators to bias the integrated-optic amplitude modulators to minimum optical transmission; a trigger delay module that provides a low-jitter, programmable delay with respect to an electrical input trigger signal.

The AWG produces longer pulses (1 to 10 ns) required for OMEGA EP that cannot be produced by the ACSL pulse-shaping system. In this device, impulses are combined at <100-ps intervals. The voltage level of each impulse is computer controlled to provide user-determined pulse shapes. The pulse shape of each beamline and the timing are independent to provide greater experimental flexibility.

2.4.3 Regenerative Amplifier

Shaped optical pulses are amplified to 2 to ~5 mJ using a diode-pumped Nd:YLF regenerative amplifier (regen), as shown in Fig. 2.15. The regen was originally developed for OMEGA but has been modified to allow pulses to be amplified with a 10-ns duration. The regen operates in a Q -switched, cavity-dumped mode to produce high gain. Along with diode pumping, gain saturation in a laser cavity with a high gain-to-loss ratio ensures highly stable operation and insensitivity to input energy fluctuations. A Faraday isolator protects the pulse-shaping system from high-intensity leakage from the regen. The Nd:YLF active element is located near the center of the laser cavity to prevent pulse overlap and the resulting spatial hole burning that can lead to pulse distortion. The active element is pumped by a single-pump diode beam that can be aligned to match the mode of the pump to that of the cavity. The intracavity Pockels cell provides Q -switching to hold off the gain of the active element and cavity dumping to release the pulse from this system.



G7233J1

Figure 2.15

Layout of the diode-pumped, cavity-dumped Nd:YLF regen. The highly stable regen amplifies shaped pulses of up to 10-ns duration to >5 mJ. The long-pulse diode-pumped regenerative (LPDR) amplifier is assembled on a ULE glass base plate and coupled to an optical table using wire flexure mounts. (See LPDR FDR, T-DR-M-250.)

2.4.4 Stimulated Brillouin Scattering

High-intensity laser light causes nonlinear generation of acoustic waves via SBS in optics. This undesirable effect is particularly threatening in the UV long-pulse optics, especially with the final focusing lenses. At high levels of SBS, the resulting acoustic wave can cause catastrophic damage to the optics.⁸ Phase modulating the pulse in the front end frustrates the phase-matching conditions needed for SBS. A bulk LiNbO₃ phase modulator of OMEGA design⁵ adds FM bandwidth to the laser pulse. An FM bandwidth of ~ 0.5 Å, generated using a 3-GHz modulation frequency, is sufficient to suppress SBS generation.¹⁴ For additional information, see “OMEGA EP SBS Suppression and Fail Safe System,” T-SS-M-006.

2.5 COMMON FRONT-END STAGING

Where possible, the laser-sources subsystems are common to both the long-pulse and short-pulse front ends to minimize system complexity and cost. Identical subsystems are used to accomplish the spatial beam shaping. The same final stage of amplification is used in either configuration.

2.5.1 Spatial Beam Shaping

The input to the OMEGA EP main amplifiers must be spatially shaped to compensate for nonuniform spatial gain effects in the main amplifiers. Beam shaping is accomplished with pixilated apodizers and masks.¹⁵ Programmable spatial light modulators¹⁶ are also being evaluated to determine if they can improve beam-shaping quality and operational flexibility for the wide range of OMEGA EP operating conditions. For example, the additional control afforded by programmable beam shaping might enable the optimization of fill factors in the main amplifiers at a variety of gain settings.

2.5.2 Glass Amplification

A large-aperture glass amplifier accepts seed pulses from either the short-pulse or long-pulse front end. Here, the pulse is amplified to energy capable of seeding the beamlines. A four-pass design provides the energy without the added space consumption of an amplifier chain. Large-aperture, 15-cm disk amplifiers are used in beamlines 1 and 2, despite the modest gain, to prevent *B*-integral accumulation. Beamlines 3 and 4 use a time-expanded ring amplifier (TERA) with a 40-mm rod amplifier head. The TERA design builds on the large-aperture ring amplifier (LARA) design principles and experience of OMEGA. After the glass amplifier, a passive isolation stage is utilized to prevent back-reflection damage to the front-end laser sources.

2.6 DIAGNOSTICS

Successful production of the required pulses in the front-end area depends on all of the subsystems operating within specifications. A variety of diagnostics are used to monitor all stages of the front-end system, ensure optimum operation, maintain a record of performance, and identify systemic problems. Many of these diagnostics record data continually during system operation. In addition, a suite of diagnostic instruments collectively referred to as the input sensor package (ISP) characterize the pulse injected into the transport spatial filter. Most of the diagnostic instruments are computer controlled, and all relevant experimental shot and test data are stored in an electronic database for later analysis.

2.6.1 Short-Pulse Oscillator

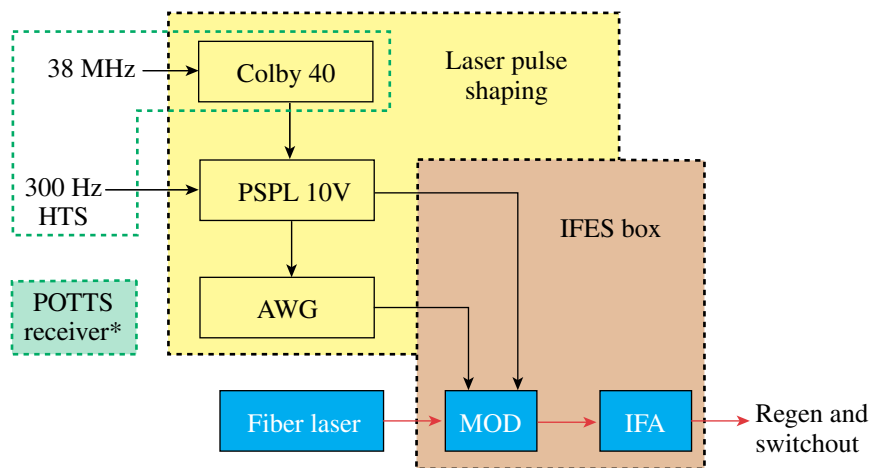
The output pulse of the short-pulse oscillator (SPO) is characterized with three commercially available instruments. A spectrometer determines the center wavelength, spectral width, and spectral shape. A power meter measures the output power of the SPO. And, an autocorrelator is used to quantify the pulse duration and the temporal shape.

2.6.2 Optical Parametric Chirped-Pulse Amplification

The energy and spectrum of the pulse generated by the OPCPA system are measured using an energy detector and spectrometer, respectively. These measurements are used to confirm the proper functioning of the OPCPA system. The compressed pulse width is diagnosed using a time-expanded-single-shot autocorrelator (TESSA) located in the short-pulse diagnostic package (SPDP). The TESSA uses pulse-front tilt and anamorphic imaging to improve performance. The pulse width is derived from the measured second-order intensity autocorrelation of a single pulse. See Chapter 6, Laser Diagnostics, S-AD-M-010, for additional information on the TESSA and other related ultrafast temporal diagnostics.

2.6.3 Monomode Oscillator

The mode, wavelength, and energy of the monomode oscillator (Sec. 2.4.1) greatly affects the performance of the laser system. The diagnostics for the subsystem shown in Fig. 2.16 include a wavelength meter and a waveform oscilloscope measuring the oscillator output and sliced pulse shapes. These diagnostics are computer controlled, and the measurements are displayed to the system operator.



*Precision POTTs triggering will replace the initial implementation that uses HTS/38 MHz triggering.

G7234J1

Figure 2.16

The seed laser is a highly stable, single-wavelength fiber laser. The output from the seed laser enters the IFES box for pulse shaping. The IFES box contains the dual-amplitude modulator (MOD), and an IFES fiber amplifier (IFA) that boosts the shaped-pulse energy before injection into the regen.

2.6.4 Input Sensor Package

The input sensor package (ISP) characterizes pulses injected into the main amplifiers. It samples full-energy pulses at the output of the glass amplifier using a pickoff. The pulse energy and the spatial and temporal profiles are measured. The beam energy is measured using an integrating-sphere design similar to the harmonic energy diagnostic used at the output of the OMEGA system.¹⁸ Within the sphere, reflected energy is uniformly distributed on the surface. An optical fiber accepts a small portion of the energy and transports it to a CCD system where the fiber tip is imaged onto a CCD camera for pixel summation. This energy diagnostic is calibrated using a full-aperture calorimeter at the final image plane of the source area or using 5-Hz probes at intermediate stages. The calorimeter is mounted on a two-state translation stage and is removed for laser shots. The spatial profile is measured using a scientific-grade CCD camera at an image plane of the front end. As on OMEGA, the temporal pulse shape is measured with a fiber-coupled streak camera.

2.6.4.1 Temporal Pulse Shape

The amplitude modulators used for temporal pulse shaping (Sec. 2.4.2) are equipped with two integrated optical sample ports. One sample is taken before the modulators for system troubleshooting. The other port samples the modulator output. This pulse is converted to an electrical waveform and displayed on a high-bandwidth, digital-sampling oscilloscope. The oscilloscope output is used for manual and computer-automated AWG adjustment of the pulse shape to meet the experimental design requirement. An infrared version of a streak camera used on OMEGA¹⁷ provides high-resolution pulse-shape and timing data at the input to the glass amplifiers.

Predicted on-target pulse shapes are calculated from the streak-camera traces using a model of the laser system that includes laser gain saturation and frequency conversion. A single streak camera monitors the pulses from all four long-pulse systems and from the two short-pulse systems. The presence of SBS-suppression bandwidth (see Sec. 2.4.4) is determined before the shot to ensure safe laser operation. This is accomplished using a high-resolution spectrometer. If the required bandwidth is not present, the subsequent pulses are prevented from propagating.

2.6.4.2 Spatial Beam Shape

Spatial profiles of the laser pulse are measured using scientific-grade charge-coupled device (CCD) cameras located at image planes in the pulse path. The images captured on the CCD camera are used to analyze the time-integrated energy distribution in the pulse. Software analysis of an image taken at the output of the glass 15-cm disc amplifier is used to verify the desired spatial pulse shape.

2.6.4.3 Alignment Sensor Package

A beam path can be uniquely determined by a location in space (centering) and a direction of propagation (pointing). The alignment sensor package (ASP), a standardized pointing and centering diagnostic, is placed before critical systems to diagnose small changes in beam alignment and enables system operators to correct for misalignment using a set of motorized mirrors. ASP diagnostics are located at the grating pulse stretcher, each crystal stage in the OPCPA, regen, CLARA, the phase-modulation crystals, the beam-shaping modules, the glass 15-cm disc amplifier, ISP, and the injection point into the main beamlines.

2.7 TIMING SYSTEMS AND FIDUCIAL LASER

2.7.1 Timing and Long-Pulse Fiducial

Laser pulses originating in the OMEGA system provide precision timing references to the laser and experimental system diagnostics of both OMEGA and OMEGA EP. Fiducial pulses are provided at the fundamental and the second and fourth harmonics of the 1053-nm source. The fiducial pulse train is a 3.8-ns-long comb of eight pulses with a period of approximately 500 ps. This pulse train is generated in parallel with the OMEGA long pulses and provides timing signals to the OMEGA EP Laser Sources Bay in time to make a determination of the timing of the laser sources output pulses in the IR ROSS camera. The fiducial pulse is timed by the gate of a pulse-shaping Pico Second Pulse Labs (PSPL) 10-V box separate from the HTS. It has a ~20-ps-rms jitter synchronization with the long-pulse output of OMEGA and OMEGA EP. For short pulses and high-resolution diagnostics, this system is inadequate at meeting jitter requirements. This fiducial is used for long-pulse synchronization only; for short-pulse synchronization, there is a separate trigger distribution and fiducial available (POTTS, see next section). The POTTS system provides a limited number of triggers that require picosecond-class jitter and resolution and is also used to synchronize OMEGA laser drivers to those of OMEGA EP and to provide high-precision synchronization of the OMEGA EP long-pulse sources to each other.

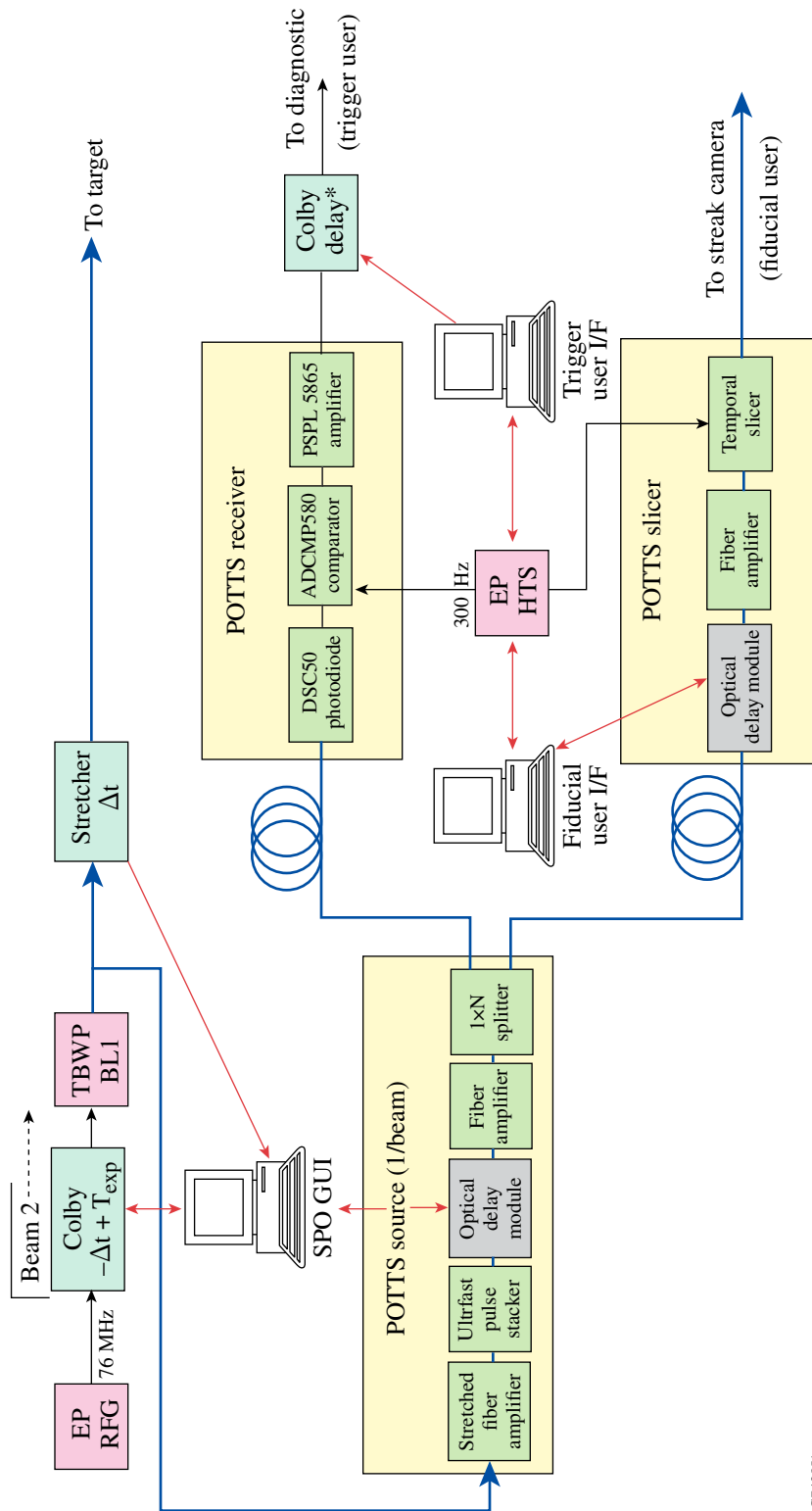
2.7.2 Precision Optical Triggering and Timing System (POTTS)

The POTTS¹⁹ will supplement the HTS by providing precision triggers or timing reference signals to a small number of subsystems that require higher resolution and lower jitter than the HTS provides. The POTTS synchronizes the short-pulse from OMEGA EP to the OMEGA drive beams on joint shots and provides a fiducial packet and/or trigger for the instruments that diagnose all short-pulse shots.

The POTTS uses a 76-MHz optical signal provided by the short-pulse oscillator in OMEGA EP's short-pulse beamline that is synchronized to the reference frequency generator (OMEGA EP-RFG), to generate the timing signal packet in the POTTS source (see Fig. 2.17). This signal packet is synchronized by the POTTS source to compensate for physical delay changes in the laser sources pulse stretcher that is necessary for pulse-width changes for a specific shot or campaign. The ROSS streak camera is also provided with an additional optical channel for use as a timing fiducial. This signal will be created using the POTTS slicer. The combination of the source, receiver, and slicer constitute the POTTS.

Changing short-pulse widths in OMEGA EP requires that the stretcher be adjusted in laser sources. This adjustment causes a time shift in the pulse propagating through the remainder of the beamline. In order to compensate for this timing change, the stretcher offset will be precompensated by advancing the locking frequency of the short-pulse oscillator with a Colby timing-delay box. The POTTS signal is picked off after precompensation but prior to the stretcher. Therefore, a delay in POTTS is required in order to match the stretcher delay that is precompensated in the Colby delay box. The POTTS source takes the 76-MHz pulse train from the short-pulse oscillator and turns them into 300-ps pulse packets. In the POTTS source, an optical delay module (ODM) is used to match the time delay induced by moving the stretcher.

The receiver converts the 300-ps pulse packets created by the source into electrical signals capable of triggering the diagnostic equipment. Electrical conversion requires converting the 76-MHz optical



G7428J1

Figure 2.17
Schematic diagram of the Precision Optical Timing and Triggering System (POTTS).

pulse train into a 76-MHz electrical pulse train, selecting a single pulse from the electrical pulse train via a trigger from the HTS, and conditioning the signal to become a 4-V, 300-ns pulse. A Colby delay box follows the receiver for additional precision-timing adjustments.

The POTTTS control system consists of three user interfaces, one each for the source, receiver (trigger user), and slicer (fiducial user). Software controls for the source are integrated into the short-pulse oscillator, graphical user interface (SPO-GUI) software application that controls the short-pulse oscillator. This software application interfaces to the Colby delay box located after the RFG, the stretcher, and the optical delay module (ODM) located in the POTTTS Source. A second application provides control software to adjust optical-timing delays for the ROSS streak camera. This application provides an interface to the HTS and the ODM located in the POTTTS slicer. A third application provides control software to adjust timing delays for diagnostics. This application provides an interface to the HTS and the Colby delay box located after the POTTTS receiver. The streak camera requires a single optical packet for timing information. The POTTTS slicer, triggered by the HTS, will select a single pulse packet from the 76-MHz optical train that includes an ODM for precise timing adjustments.

2.8 REFERENCES

1. I. N. Ross, P. Matousek, M. Towrie, A. J. Langley, and J. L. Collier, “The Prospects for Ultrashort Pulse Duration and Ultrahigh Intensity Using Optical Parametric Chirped Pulse Amplifiers,” *Opt. Commun.* **144**, 125 (1997).
2. I. N. Ross, J. L. Collier, P. Matousek, C. N. Danson, D. Neely, R. M. Allott, D. A. Pepler, C. Hernandez-Gomez, and K. Osvay, “Generation of Terawatt Pulses by Use of Optical Parametric Chirped Pulse Amplification,” *Appl. Opt.* **39**, 2422 (2000).
3. “The Design of Optical Pulse Shapes with an Aperture-Coupled-Stripline Pulse-Shaping System,” *LLE Review Quarterly Report* **78**, 97, Laboratory for Laser Energetics, University of Rochester, Rochester, NY, LLE Document No. DOE/SF/19460-295 (1999).
4. A. V. Okishev, D. J. Battaglia, I. A. Begishev, and J. D. Zuegel, “Highly Stable, Diode-Pumped, Cavity-Dumped Nd:YLF Regenerative Amplifier for the OMEGA Laser Fusion Facility,” in *OSA TOPS Vol. 68, Advanced Solid-State Lasers*, edited by M. E. Fermann and L. R. Marshall, OSA Technical Digest (Optical Society of America, Washington, DC, 2002), p. 418.
5. “Microwave Phase Modulators for Smoothing by Spectral Dispersion,” *LLE Review Quarterly Report* **68**, 192, Laboratory for Laser Energetics, University of Rochester, Rochester, NY, LLE Document No. DOE/SF/19460-139, NTIS Order No. DE97002520 (1996). (Copies may be obtained from the National Technical Information Service, Springfield, VA 22161.)
6. M. D. Martinez, K. M. Skulina, F. J. Deadrick, J. K. Crane, B. Moran, J. Braucht, B. Jones, S. Hawkins, R. Tilley, J. Crawford, D. Browning, and F. Penko, “Performance Results of the High Gain, Nd:Glass, Engineering Prototype Preamplifier Module (PAM) for the National Ignition Facility (NIF),” Lawrence Livermore National Laboratory, Livermore, CA, UCRL-JC-132679 (1999).

7. A. Babushkin, J. H. Kelly, C. T. Cotton, M. A. Labuzeta, M. O. Miller, T. A. Safford, R. G. Roides, W. Seka, I. Will, M. D. Tracy, and D. L. Brown, "Compact Nd³⁺-Based Laser System with Gain $G \leq 10^{13}$ and Output Energy of 20 J," in *Third International Conference on Solid State Lasers for Application to Inertial Confinement Fusion*, edited by W. H. Lowdermilk (SPIE, Bellingham, WA, 1999), Vol. 3492, p. 939.
8. J. R. Murray, J. R. Smith, R. B. Ehrlich, D. T. Kyrakis, C. E. Thompson, T. L. Weiland, and R. B. Wilcox, "Experimental Observation and Suppression of Transverse Stimulated Brillouin Scattering in Large Optical Components," *J. Opt. Soc. Am. B* **6**, 2402 (1989).
9. D. Kopf, F. X. Kartner, D. Keller, and K. J. Weingarten, "Diode-Pumped Mode-Locked Nd:Glass Lasers with an Antiresonant Fabry–Perot Saturable Absorber," *Opt. Lett.* **20**, 1169 (1995).
10. G. Chériaux, P. Rousseau, F. Salin, J. P. Chambaret, B. Walker, and L. F. Dimauuro, "Aberration-Free Stretcher Design for Ultrashort-Pulse Amplification," *Opt. Lett.* **21**, 414 (1996).
11. D. Du, J. Squier, S. Kane, G. Korn, G. Mourou, C. Bogusch, and C. Cotton, "Terawatt Ti:Sapphire Laser with a Spherical Reflective-Optic Pulse Expander," *Opt. Lett.* **20**, 2114 (1995).
12. S. K. Zhang, M. Fujita, M. Yamanaka, M. Nakatsuka, Y. Izawa, and C. Yamanaka, "Study of the Stability of Optical Parametric Amplification," *Opt. Commun.* **184**, 451 (2000).
13. E. Hecht, *Optics*, 3rd ed. (Addison-Wesley, Reading, MA, 1998), p. 191.
14. M. Bowers and J. Murray, Lawrence Livermore National Laboratory, private communication (2002).
15. S. C. Burkhart, R. J. Beach, J. H. Crane, J. M. Davin, M. D. Perry, and R. B. Wilcox, "The National Ignition Facility Front-End Laser System," in *First Annual International Conference on Solid State Lasers for Application to Inertial Confinement Fusion*, edited by M. André and H. T. Powell (SPIE, Bellingham, WA, 1995), Vol. 2633, p. 48.
16. K. A. Bauchert, S. A. Serati, G. D. Sharp, and D. J. McKnight, "Complex Phase/Amplitude Spatial Light Modulator Advances and Use in a Multispectral Optical Correlator," in *Optical Pattern Recognition VIII*, edited by D. P. Casasent and T.-H. Chao (SPIE, Bellingham, WA, 1997), Vol. 3073, p. 170.
17. "A Self-Calibrating, Multichannel Streak Camera for Inertial Confinement Fusion Applications," *LLE Review Quarterly Report* **87**, 109, Laboratory for Laser Energetics, University of Rochester, Rochester, NY, LLE Document No. DOE/SF/19460-397, NTIS Order No. PB2006-106658 (2001). (Copies may be obtained from the National Technical Information Service, Springfield, VA 22161.)

18. “A Novel Energy Measurement System for the OMEGA Laser,” *LLE Review Quarterly Report* **63**, 110, Laboratory for Laser Energetics, University of Rochester, Rochester, NY, LLE Document No. DOE/SF/19460-91, NTIS Order No. DE96000767 (1995). (Copies may be obtained from the National Technical Information Service, Springfield, VA 22161.)
19. Precision Optical Triggering and Timing System TRD: D-AA-R-031; Precision Optical Triggering and Timing System Software Control Requirements, C-AM-R-006; Precision Optical Timing & Triggering System (POTTS) PDR, C-AM-M-013.

Appendix A
Glossary of Acronyms

ACSL	Aperture-coupled strip line
AE	Active element (temperature control)
AFC	Amplifier facility controller
ASE	Amplified spontaneous emission
ASP	Alignment sensor package
AWG	Arbitrary waveform generator
BL	Beamline
CCD	Charge-coupled device
CLARA	Crystal LARA (large-aperture ring amplifier)
Colby	Colby Instruments, Inc. (delay or phase-shifting devices)
DFB	Distributed feedback (laser)
FI	Faraday isolator
FM	Frequency modulated
FR	Faraday rotator
FW	Full width
FWHM	Full width at half maximum
GUI	Graphical user interface
GW	Gigawatt
HTS	Hardware Timing System
IFA	IFES (integrated front-end source) fiber amplifier
IFES	Integrated front-end source
IR	Infrared
IRAT	Infrared alignment table
ISP	Input sensor package
KDP	Potassium dihydrogen phosphate
$\lambda/2$	Half-wave plate
$\lambda/4$	Quarter-wave plate
LARA	Large-aperture ring amplifier
LBO	Lithium triborate
LiB_3O_5	Lithium triborate
LiNbO_3	Lithium niobate
LLE	Laboratory for Laser Energetics
LLNL	Lawrence Livermore National Laboratory

Final Draft

LP	Long pulse
LPDR	Long-pulse diode-pumped regenerative (amplifier)
MOD	Dual-amplitude modulator
MOPA	Master-oscillator, power-amplifier
Nd	Neodymium
NIF	National Ignition Facility
ODM	Optical-delay module
OPA	Optical parametric amplifier
OPCPA	Optical parametric chirped-pulse amplification
OSA	Optical-spectrum analyzer
OTDR	Optical time-delay reflectometry
PC	Pockels cell
Pol	Polarizer
POTTS	Precision optical timing trigger system
ps	Picosecond
PSPL	Picosecond Pulse Labs
p-v	Peak-to-valley
PZT	Piezoelectric transducer
RFG	Reference-frequency generator
rms	Root mean square
ROSS	Rochester Optical Streak System
SBS	Stimulated Brillouin scattering
SESAM	Semiconductor saturable absorbing mirror
SHG	Second-harmonic generator
SLM	Single-longitudinal mode
SPO	Short-pulse oscillator
SPDP	Short-pulse diagnostic package
TBWP	Time-bandwidth product
TEC	Thermoelectric cooler
TERA	Time-expanded ring amplifier
TESSA	Time-expanded-single-shot autocorrelator
TRD	Technical Requirements Document
TSF	Transport spatial filter
ULE	Ultralow expansion glass (Corning, Inc.)
UTD	Ultrafast-temporal diagnostic
YLF	Ytterbium lithium fluoride